Sensor and Simulation Notes
Note 468

Improved Aperture Efficiency in IRAs and ORAs with Uniaxially Conducting Reflectors

J. Scott Tyo
Electrical and Computer Engineering Deparment
University of New Mexico
Albuquerque, NM 87131-1356
tyo@eece.unm.edu

May 2002

Abstract

Wideband, focused apertue antennas like impulse radiating antennas (IRAs) and oscillator reflector antennas (ORAs) can see improved aperture efficiency through control of the aperture fields and aperture shape. It has been suggested recently that the aperture efficiency can be further improved by reshaping the aperture fields through the use of uniaxially conducting reflectors, e.g. reflectors made of conducting wires rather than solid sheets. In this paper, the benefit that can be obtained by using this strategy is explored analytically. Optimum filament orientation are show, and the improvements possible in coplanar plate-fed IRAs and ORAs are presented. For common antenna configurations and impedances, the aperture height can be increased by amounts ranging from 7% to 67%. A method for extending the concept to lens IRAs is also proposed.

This work was supported in part by the Air Force Office of Scientific Research under the MURI program.

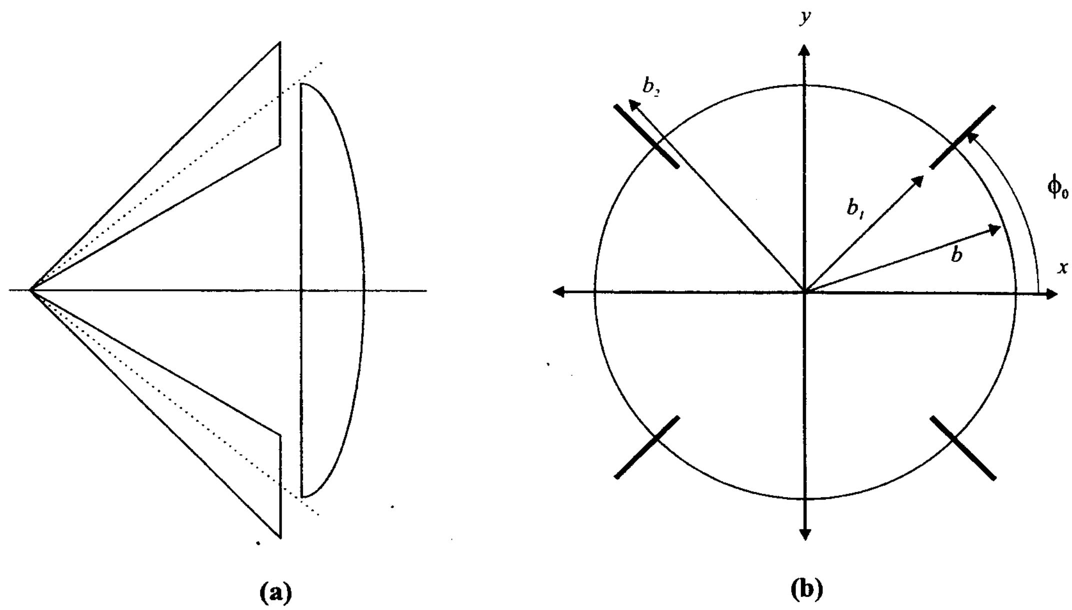

Figure 1: Schematic diagram of IRAs and ORAs. The source is at the apex of the TEM feed line. This diagram is for reflector antennas, but the focusing optic could also be a lens [1]. A. Side view. B. Aperture plane (after stereographic projection).

1 Introduction

Impulse radiating antennas (IRAs) [1] and oscillator reflector antennas (ORAs) [2] belong to the class of focused aperture antennas. These antennas are particularly well suited for radiating energy generated by spark gap switches. The general configuration of an IRA or ORA is depicted in fig. 1. The concept behind the antenna operation is that a spherical wave is launched by the source onto the nondispersive TEM transmission line feed structure of characteristic impedance Z_{line}. That spherical wave is converted into a plane wave in the geometric optics approximation by the focusing optic. The focusing optic can be a lens or a reflector (or even a timed array), but for many practical application, reflectors are preferable for their light weight and low volume [3]. Aperture theory (physical optics) is then used to compute the radiated far field. It is well known that the prompt field from an IRA in the direction of focus is given approximately as

$$E_{rad} = \frac{h_a}{2\pi r c f_g} \frac{dV}{dt}, \tag{1}$$

where V is the applied voltage waveform, r is the distance to the observation point, c is the speed of light, $f_g = Z_{line}/\eta_0$, and h_a is the aperture height given by

$$h_a = -\frac{f_g}{V_0} \int\!\!\int_A E_y(x,y)\,dx\,dy. \tag{2}$$

The quantity V_0 in (2) is the peak applied voltage, and the surface integral in (2) is carried out over the extent of the focused aperture. In general h_a is a convlution operator in time, but for early times the voltage on the line and electric field in the aperture have the same temporal dependence and h_a can be considered constant. At later times, the fields in the aperture can be modified from the transmission line approximation. Strictly speaking, the aperture height is a vector quantity, with the x-component computed in the same fashion, but the symmetry of most practical IRAs forces the x-component of h_a to be zero [1].

A concept of prompt aperture efficiency has been introduced for time-domain aperture antennas like IRAs and ORAs [4], and it was shown that typical reflector IRAs with the feed arms oriented at angles of 45° with respect to the horizontal have aperture efficiencies on the order of 25%. The low aperture efficiency is due to two primary factors. First, a significant amount of power carried on the TEM feed line is propagating in fields that miss the focusing optic – an effect equivalent to spillover. Exactly 50% of the power misses the optic in IRAs fed by self reciprocal feed structures [5]. The second mechanism that reduces the aperture efficiency is field nonuniformity, which is inherent in all TEM modes on balanced transmission lines.

Several studies have explored mechanisms to increase aperture efficiency by addressing some of these issues. Buchenauer, *et al.* [4] showed that low-impedance, flat-plate TEM horns have aperture efficiencies that approach unity, but this type of feed is not suitable for use with reflectors. Tyo predicted numerically that moving the feed arms towards the vertical would increase field uniformity, providing a substantial increas in aperture efficiency [6]. These results were verified experimentally by Bowen, *et al.*, for reflector IRAs with feed arms at 60° from the horizontal [7]. Baum suggested that removal of portions of the aperture where E_y has the wrong sign from the integral in (2) could increase the aperture efficiency. This theory was verified numerically and experimentally by Baretela and Tyo [8]. Baretela and Tyo also showed that the aperture efficiency could be further improved by decreasing the size of the feed structure relative to the reflector and then trimming the resulting aperture accordingly [8]. All of these modification can improve the performance of an IRA or ORA without modifying the input impedance, and these changes do not affect the upstream components of the system.

2 REORIENTING THE APERTURE FIELDS

Baum has suggested recently that the aperture efficiency can be further increased by actually reorienting the fields in the aperture plane [9]. This can be accomplished by replacing the solid reflector with a mesh that conducts uniaxially. The solid reflector will carry current parallel to the local electric field, but the uniaxially conducting reflector can only carry currents along the direction of the wire. To maximize the response from the antenna, the direction of current flow at each point on the aperture should bisect the angle between the local tangential electric field and the vertical direction as shown in fig. 2.

The early-time vector electric field of the TEM mode in the aperture plane can be derived from a complex scalar potential as follows. The complex coordinate is $z = x + jy$, and the complex potential is $w = u + jv$. The electric scalar potential is u and the magnetic scalar potential is v. The complex electric field is then [1]

$$E = E_x - jE_y = \frac{dw}{dz} = -\frac{du}{dx} + j\frac{du}{dy}. \qquad (3)$$

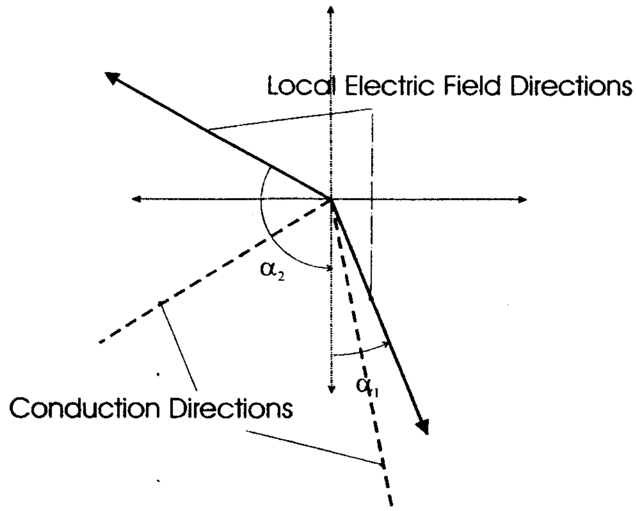

Figure 2: Two examples of the local conduction direction given the local electric field. The conduction direction bisects the angle α between the local electric field and the negative y-direction.

Define the angle α from fig. 2 as

$$\alpha = \tan^{-1}\frac{E_x}{-E_y}, \tag{4}$$

and the unit vector $\hat{\ell}$ that gives the desired direction of local current flow is

$$\hat{\ell} = \sin\frac{\alpha}{2}\hat{\mathbf{x}} - \cos\frac{\alpha}{2}\hat{\mathbf{y}}. \tag{5}$$

The resulting current flow is proportional to $(\mathbf{E}\cdot\hat{\ell})\hat{\ell}$, and the y-component is

$$J_y \propto -E_x \sin\frac{\alpha}{2}\cos\frac{\alpha}{2} + E_y\cos^2\frac{\alpha}{2} \tag{6}$$

$$\propto -\frac{1}{2}E_x\sin\alpha + E_y\frac{1+\cos\alpha}{2}. \tag{7}$$

Since $\sin\alpha = E_x/\sqrt{E_x^2+E_y^2}$ and $\cos\alpha = -E_y/\sqrt{E_x^2+E_y^2}$, (7) becomes

$$J_y \propto \frac{1}{2}\left[-\frac{E_x^2+E_y^2}{\sqrt{E_x^2+E_y^2}} + E_y\right] = \frac{1}{2}(E_y - |\mathbf{E}|). \tag{8}$$

The resulting quantity is always nonpositive, and is largest (most negative) when $\mathbf{E} = E_y\hat{\mathbf{y}}$ with E_y negative. The negative sign results from the fact that the top half of the TEM feed is usually taken as having positive voltage. The current flow on the wires is zero only at locations where $\mathbf{E} = E_y\hat{\mathbf{y}}$ with E_y positive. This strategy represents an improvement over the aperture trimming proposed by Baum [9] and Baretela and Tyo [8] because essentially all portions of the aperture can be made to contribute constructively to the surface integral in (2).

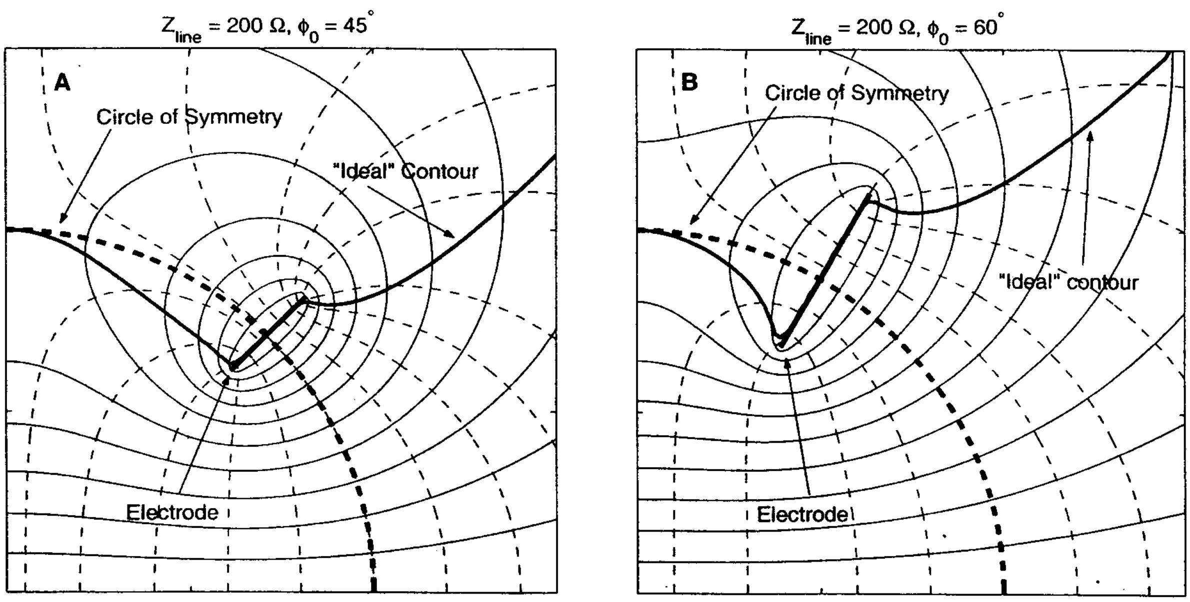

Figure 3: Potential (solid lines) and field distributions (dashed lines) for 200-Ω IRAs and ORAs with A. $\phi_0 = 45°$ and B. $\phi_0 = 60°$. Note that the circle of symmetry of the feed structure is also a field line [5]. The ideal contour indicated in the figures is the contour where $E_y = 0$. Trimming the portions of the aperture above this contour was shown to increase h_a [8].

3 LOCAL CURRENT DIRECTIONS

The local direction of conduction is determined by computing the TEM mode distribution in the aperture plane and projecting that onto the paraboloidal surface through a stereographic projection. We will consider only the aperture plane here for simplicity (i.e. no stereographic projection has been performed). The potential and field distribution for one quadrant of 200-Ω-impedance reflector IRAs with feed arms at 45° and 60° from the horizontal are depicted in fig. 3. The antenna with the 60° feed arms is significantly more aperture efficient than the antenna with the 45° feed arms when the circle of symmetry coincides exactly with the focused aperture. The increased efficiency is due to the fact that the fields are more uniform (and less of the aperture contributes destructively to the aperture integral) [8]. The appropriate conducting paths are indicated for these two cases in fig. 4.

4 IMPROVEMENT IN APERTURE HEIGHT

The aperture efficiency is given in terms of the aperture height as [4, 6]

$$\eta_A = \frac{h_a^2}{f_g A}. \tag{9}$$

When the input impedance (f_g) is fixed and the aperture is circular with radius ρ, $A = \pi\rho^2$ and η_A is maximized when h_a/ρ is maximized. This quantity is termed here as the normalized aperture

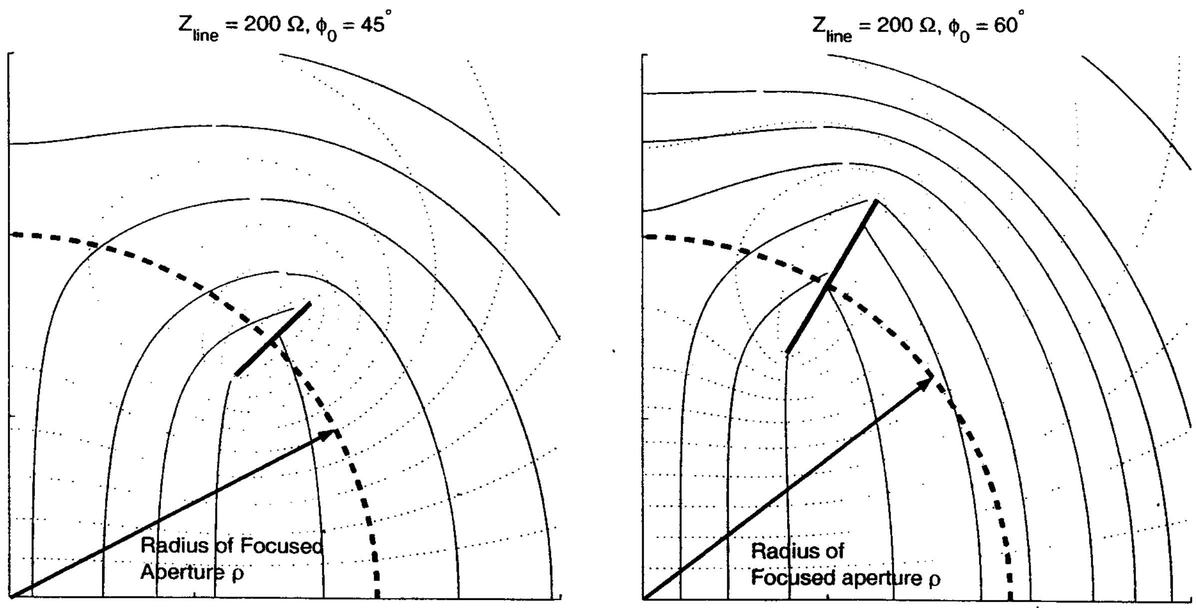

Figure 4: Local orientation of conductors for optimal aperture height. The solid lines bisect the angle between the local field direction displayed in fig. 3 and the negative y-direction as shown in fig. 2.

height and is defined as $\bar{h_a} \equiv h_a/\rho$. Fig. 5 shows the aperture height and normalized aperture height as a function of the radius of the circular aperture for 200-Ω IRAs with several feed arm angles.

Fig. 5A shows the aperture height for fixed-size feed arms as the radius of a circular aperture is increased. The solid lines show the aperture height with a solid reflector and the dashed lines show the aperture height using the uniaxially-conducting strategy outlined above. The aperture height for the solid reflector case increases until the circle intersects the outer tip of the electrode, at which point the aperture height remains constant. This result is consistent with results presented earlier [8]. The aperture height for the uniaxially conducting reflector continues to increase regardless of the size of the aperture. However, there is a clear optimum radius for a given feed arm angle as can be seen from fig. 5B. This optimum radius is significantly higher than was found by using aperture trimming alone, as is detailed in table 1. As can be seen in the table, the increase realized by using a uniaxially conducting circular reflector is significant. The smallest improvement realized was 7.7% over the solid reflector with feed arms at 60° and $Z_{line} = 100\Omega$. For the near-optimal confifuration of a 200Ω-antenna with $\phi_0 = 60°$ [6, 7], aperture trimming provides little benefit because only a small part of the aperture is removed [8]. In that case, aperture trimming provides only a 2% increase in the aperture height. The inclusion of a uniaxially conducting reflector in this configuration provides a substantial 11% increase in the aperture height. At lower feed arm angles, the improvement is much more dramatic (as much as 66% at 15° and $Z_{line} = 200\Omega$). At these low feed arm angles, aperture trimming provides a significant benefit because large portions of the aperture are removed [8]. The uniaxially-conducting reflector can provide even greater benefits, since the portions of the aperture removed by trimming are

Z_{line}	ϕ_0°	$\bar{h}_a$ - COS	$\bar{h}_{a,max}$ - trim	$\bar{h}_{a,max}$ - uni	r_{opt} - trim	r_{opt} - uni
100	60	0.443	0.453	0.477	0.97	2.00
100	45	0.439	0.457	0.497	1.58	1.80
100	30	0.372	0.433	0.463	1.62	1.60
100	15	0.226	0.326	0.361	1.34	1.35
150	75	0.584	0.589	0.646	0.89	1.70
150	60	0.616	0.623	0.681	1.13	1.50
150	45	0.571	0.610	0.676	1.31	1.40
150	30	0.437	0.521	0.575	1.26	1.29
150	15	0.243	0.347	0.405	1.24	1.25
200	75	0.726	0.730	0.805	0.96	1.44
200	60	0.736	0.750	0.821	1.11	1.26
200	45	0.648	0.687	0.799	1.16	1.20
200	30	0.480	0.559	0.637	1.14	1.22
200	15	0.254	0.355	0.419	1.16	1.23
250	75	0.841	0.845	0.917	0.96	1.23
250	60	0.812	0.828	0.890	1.09	1.15
250	45	0.678	0.719	0.800	1.09	1.16

Table 1: Comparison between solid reflector, optimally trimmed reflector, and optimal uniaxially conducting reflector. The third column gives $\bar{h}_a$ for a circular aperture at the circle of symmetry of the feeds with no modifications to the reflector. The fourth column gives the optimum $\bar{h}_a$ for a trimmed aperture. The fifth column gives the optimum $\bar{h}_a$ for a uniaxially conducting aperture. The last two columns give the optimum radius for the trimmed and uniaxially conducting reflectors, respectively. Note that *substantial* performance improvements are possible with the uniaxially conducting reflectors. For common configurations, the improvement is on the order of 20%. Also note that the optimum radius for uniaxially conducting reflectors is usually much larger than the circle of symmetry or the optimum radius for trimmed apertures.

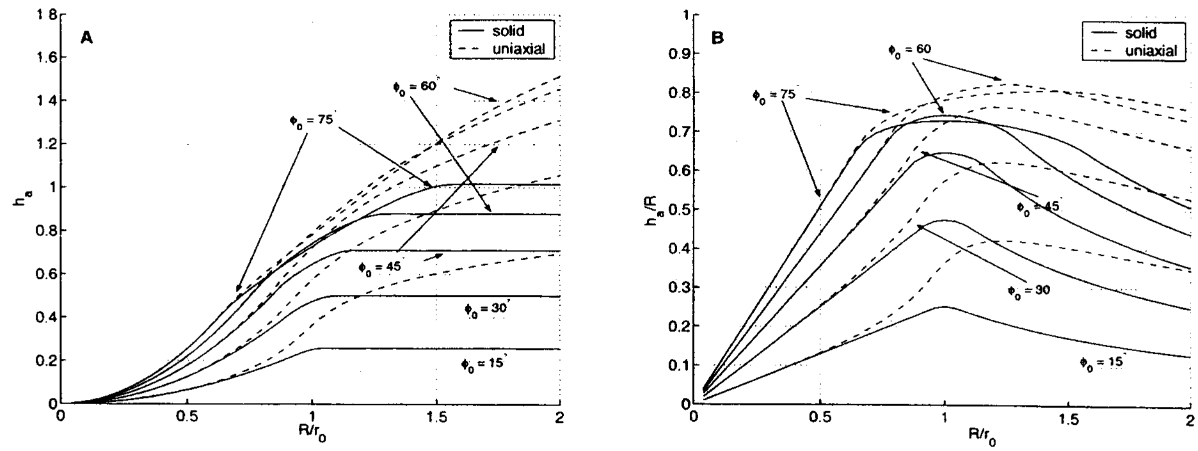

Figure 5: Aperture height and normalized aperture height for $Z_{line} = 200\Omega$ at a variety of feed angles ϕ_0. A. h_a as a function of radius for solid reflectors (solid lines) and uniaxially conducting reflectors (dashed lines). R is the radius of the circular aperture and r_0 is the radius of the circle of symmetry of the TEM feed structure. The aperture height flattens at the outer edge of the feed arms for the solid reflector, but continues to increase for the modified reflector. B. $\bar{h}_a$ as a function of radius. $\bar{h}_a$ has a clear optimum for all angles, and the improvement possible with the modified reflector is greater than 10% in all cases.

made to contribute to the aperture height.

The detailed results for the $Z_{line} = 200\Omega$ are presented above because that is the most common impedance used in high power applications [1]. Similar calculations can also be performed for other impedances, and the results are summarized in fig. 6. Fig. 6A presents the optimum value of $\bar{h}_a$ as a function of feed arm angle for several common impedances used for IRAs and ORAs. Fig. 6B presents the circular radius that yields that maximum value of $\bar{h}_a$ as a function of ϕ_0 for each impedance.

5 APPLICATION TO LENS IRAs and ORAs

The results above demonstrate that the strategy proposed in this paper can be very beneficial in virtually all reflector IRA and ORA configurations. A further question is whether or not similar results can be achieved for lens IRAs and ORAs by using the complementary strategy. With lens IRAs, we would like to transmit the y-polarized fields through the aperture, not reflect them. In that case, the wires should be oriented at an angle that optimally reflects the unwanted fields. The angle of the wires should be $\beta/2$, where $\beta = \tan^{-1} E_y/E_x$ is the angle made by the field with respect to the positive y-direction as depicted in fig. 7. . The effect of putting such a structure in place is to reflect the unwanted fields and allow the desired fields to pass. This concept has been used extensively to fabricate linear polarizers for use at infrared wavelengths [10]. As pointed out by Baum [9], this strategy for a lens IRA is complementary to the one discussed above for reflectors.

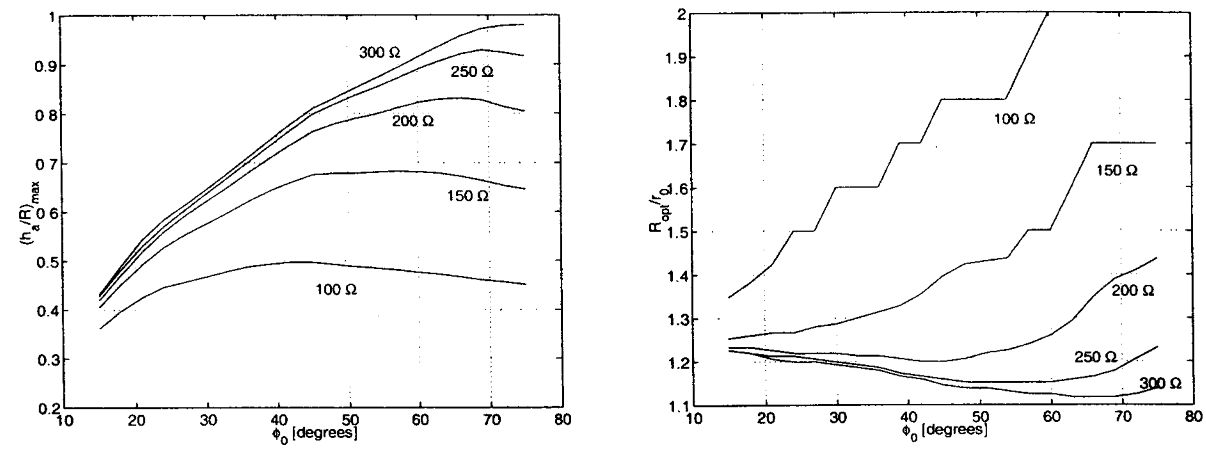

Figure 6: A. Optimum $\bar{h_a}$ as a function of feed arm angle ϕ_0 for common feed impedances. Note that the optimum angle for each feed impedance increases monotonically. B. The radius that the maximum $\bar{h_a}$ occurs at for the cases in panel A. The staircased nature of the data is due to coarse sampling. It is equivalent to either increase the size of the aperture for a fixed feed arm geometry or to decrease the size of the feed arms for a fixed maximum aperture size.

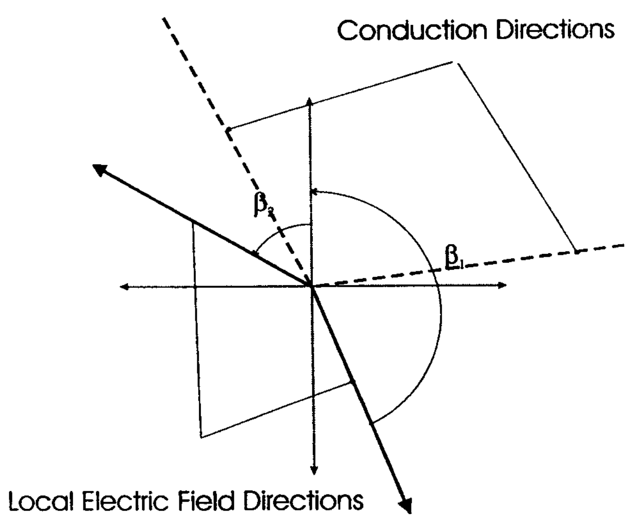

Figure 7: Conductor configuration for lens IRAs and ORAs. The local conduction direction is chosen now to reflect the *undesired* fields. This structure will act like a wire grid polarizer [10].

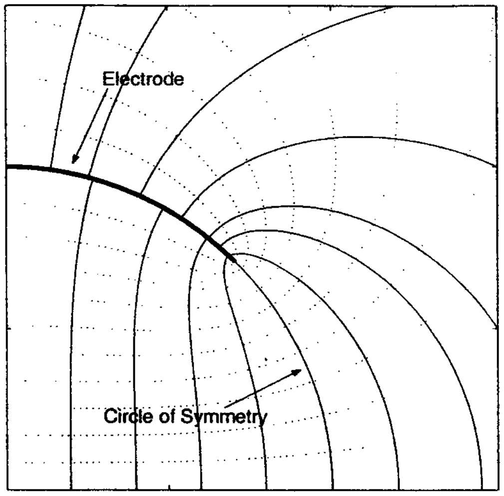

Figure 8: Field lines (solid) and potential distributions (dotted) for a circular, conical plate-fed lens IRA or ORA. This structure has $Z_{line} = 60\pi$ with the electrode tip at 45° from the vertical. The fields inside the circle of symmetry are far more uniform, and the majority of the loss of aperture efficiency is due to fields propagating outside the lens.

The feed geometries used for lens IRAs and ORAs are typically significantly more aperture efficient [4]. The reason for this can be seen in fig. 8, which depicts the potential and field distribution for a circular, conical plate-fed lens IRA. This feed geometry is still self-reciprocal, meaning that 50% of the power misses the lens, but the aperture efficiency is 46% (as compared with 25% for 200-Ω reflector IRAs with 45° feed arms [4].

Fig. 9 shows the computed values of $\bar{h}_a$ for a circular aperture that coincides with the circle of symmetry as a function of the electrode angle ϕ_0 depicted in fig. 8. Fig. 9A shows the results for the optimum orientation of the wires.

There are some practical concerns associated with this strategy that may make it difficult to implement. First, the transmission through wire grid polarizers can be low for the desired polarization state if they are not properly fabricated. Second, the undesired fields are reflected by the polarizer and will propagate back down the TEM feed to the source. This can be highly detrimental to the source lifetime, especially in high power applications. Such an effect can be potentially mitigated by fabricating the wire grid from lossy wires, in which case they might act more like a typical dichroic polarizer used at optical wavelengths, i.e. the polarizer absorbs the unwanted energy instead of reflecting it. Such a strategy can be used in conjunction with the termination that is necessary to improve the late-time response of the antenna [1].

The polarizer strategy does provide a small benefit for lens IRAs and ORAs, but the effect is nowhere near as dramatic as for reflector IRAs and ORAs. In lens IRAs, the dominant effect that reduces aperture efficiency is spillover [4]. The only method that has been proposed to reduce spillover involves the use of isorefractive materials to concentrate the power in the aperture [11]. A method has been proposed to realize such materials [12], but to our knowledge none has been fabricated as yet.

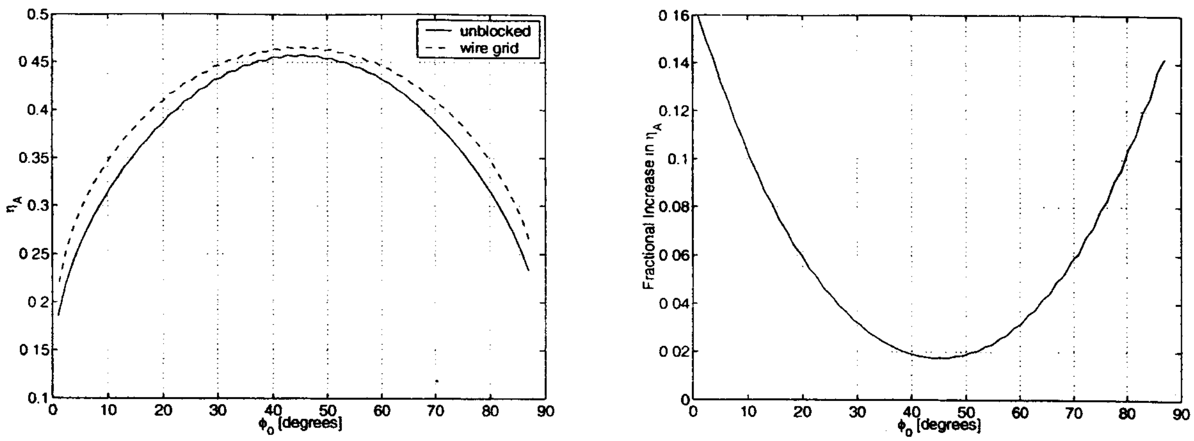

Figure 9: Aperture efficiency for lens IRAs and ORAs. A. η_A as a function of electrode angle for the wire grid (dashed) and unblocked (solid) apertures. B. Fractional improvement realized by using the polarizer.

6 DISCUSSION AND CONCLUSIONS

The results presented here clearly demonstrate that replacing the solid paraboloidal reflector with a mesh of uniaxially conducting wires has the potential to *substantially* increase the radiated fields from IRAs and ORAs. However, there are many additional factors that must be considered to determine how practical this solution is. In practice, the exact pattern necessary to achieve these ideal results can only be determined by numerical methods. In addition, a method must be devised that will allow these patterns to be synthesized while maintaining the structural integrity of the reflector.

For ORAs, the spacing of the wires can be chosen to be small compared with the center frequency as discussed by Baum [2]. The wires will appear inductive to the field, and will therefore need to be displaced by an appropriate distance from the actual paraboloidal surface in order to maintain the focusing properties of the optic. For IRAs, it is not as clear that these solutions can work. The broadband nature of the waveforms transmitted by IRAs will force the spaceing between conducting wires to be small, probably on the order of $ct_r/10$, where c is the speed of light and t_r is the risetime of the step applied to the IRA. The reflector still can be expected to ring in the late time, even with small spacing, and that will affect the transmitted response after the prompt signal.

The significant benefits predicted by this analysis seem to indicate that it's worth trying this strategy for reflector IRAs and ORAs. The late-time effects for IRAs are difficult to predict, but we hope to perform a set of experiments that will determine the feasibility of this strategy.

References

[1] C. E. Baum, E. G. Farr, and D. V. Giri, "Review of impulse-radiating antennas," in *Review of Radio Science* (W. R. Stone, ed.), pp. 403–439, New York: Oxford U. Press, 1999.

[2] C. E. Baum, "Differential switched oscillators and associated antennas," in *Sensor and Simulation Notes #457* (C. E. Baum, ed.), Albuquerque, NM: Air Force Research Laboratory, 2001.

[3] D. V. Giri, H. Lackner, I. D. Smith, D. W. Morton, C. E. Baum, J. R. Marek, W. D. Prather, and D. W. Scholfield, "Design, fabrication, and testing of a paraboloidal reflector antenna and pulser system for impulse-like waveforms," *IEEE Trans. Plasma Sci.*, vol. 25, pp. 318–326, 1997.

[4] C. J. Buchenauer, J. S. Tyo, and J. S. H. Schoenberg, "Prompt aperture efficiencies of impulse radiating antennas with arrays as an application," *IEEE Trans. Antennas Propagat.*, vol. 49, pp. 1155–1165, 2001.

[5] E. G. Farr and C. E. Baum, "Radiation from self-reciprocal apertures," in *Electromagnetic Symmetry* (C. E. Baum and H. N. Kritikos, eds.), ch. 6, pp. 281–308, New York: Plenum, 1995.

[6] J. S. Tyo, "Optimization of the TEM feed structure for four-arm reflector impulse radiating antennas," *IEEE Trans. Antennas Propagat.*, vol. 49, pp. 607–614, 2001.

[7] L. H. Bowen, E. G. Farr, C. E. Baum, T. C. Tran, and W. D. Prather, "Experimental results of optimizing the location of feed arms in a collapsible IRA and a solid IRA," in *Sensor and Simulation Notes #450* (C. E. Baum, ed.), Albuquerque, NM: Air Force Research Laboratory, 2000.

[8] M. J. Baretela and J. S. Tyo, "Selective trimming of impulse radiating apertures to increase prompt radiated fields," in *Sensor and Simulation Notes #461* (C. E. Baum, ed.), Albuquerque, NM: Air Force Research Laboratory, 2001.

[9] C. E. Baum, "Modification of TEM-fed reflector for increased efficiency," in *Sensor and Simulation Notes #458* (C. E. Baum, ed.), Albuquerque, NM: Air Force Research Laboratory, 2001.

[10] R. M. A. Azzam and N. M. Bashara, *Ellipsometry and Polarized Light*. New York: North-Holland, 1977.

[11] J. S. Tyo, C. J. Buchenauer, and J. S. H. Schoenberg, "Use of isorefractive media to improve prompt aperture efficiency in a lens IRA," *IEEE Trans. Antennas Propagat.*, vol. 46, pp. 1114–1115, 1998.

[12] J. S. Tyo, "A class of longitudinally symmetric artificial material isorefractive with free space," *IEEE Trans. Antennas Propagat.* Accepted for publication, April 2002.